Observation and Prediction of Runaway Electrons in the COMPASS Tokamak

R. Papřok

Charles University in Prague, Faculty of Mathematics and Physics, Prague, Czech Republic.

L. Krlín, J. Stöckel

Association Euratom-IPP.CR, Za Slovankou 3, Prague, Czech Republic.

Abstract. In this paper we present new measurements of HXR radiation from the COMPASS tokamak by the use of scintillation detector, 21-pinhole CdTe semiconductor detector. This radiation is caused by the presence of highly energetic runaway electrons and in the case of Neutral Beam Injection by fusion products. We also present direct runaway electrons measurements by Cherenkov detector. We present a theoretical prediction of runaway production based on theoretical formula and experimental data from Thomson scattering and compare it with a simpler experimental method based on peak counting.

Introduction

Unmitigated runaway electrons will present one of the major threats for consistency of the plasma facing components in the ITER tokamak. Up to 70 % of plasma current, electron energies up to 25 MeV and strong spacio-temporal correlation are managed to damage the first wall or the divertor dome even up to water cooling pipes. Therefore there is a large international effort to better characterize heat loads on plasma facing components and for a better understanding of runaway electron mitigation methods [*Ikeda et al.*, 2007].

The COMPASS tokamak is by its suitable size capable to enrich knowledge base at this field, especially when it would be equipped with another diagnostics, e.g. more HXR detectors to observe deposition asymmetries, IR camera for observation of runaway synchrotron radiation or SXR medical 2D camera to observe details of runaway electron interaction with PFC or diagnostic probes and mitigation tools, e.g., currently prepared magnetic perturbation coils or (multiple) fast gas valves for Massive Gas Injection.

In the present paper we describe current knowledge about runaways in the COMPASS tokamak. Firstly we describe and compare measurement results for three different diagnostics: scintillation detector, 21 pinhole array of semiconductor detectors and Cherenkov detector. Then we use these data and data from another diagnostics to compute number of runaways created during discharge, runaways current and their total and maximal energy. In the last chapter we summarize and discuss obtained results.

Description of diagnostics and experimental setup

Scintilation detector

NaI scintillation detector of HXR is routinely used at the COMPASS tokamak. The detector is unshielded and installed in a $5m$ distance from the tokamak vessel so it gives only a very limited information about energy deposition patterns. At the same time it is supposed to have good energy resolution form ≈ 100 keV up to several MeVs and detection efficiency above 90 %. Collecting area of the detector is about 5 cm^2.

21 pinhole HXR camera

The 21 pinhole HXR camera consists on an array of 21 Cadmium telluride (CdTe) semiconductor detectors. This camera was designed to measure bremsstrahlung from supra-thermal electrons in energy range 20–200 keV. The size of each CdTe detectors is 5×5 mm^2 surface area and 2 mm thickness. Stopping efficiency for the CdTe is maximal for ≈ 100 keV dropping down to the $\approx 1/5$th of the maximal value at ≈ 600 keV. The 2 cm thick lead shielding box is insufficient for $\approx$ MeV photons. More details about camera can be found in the paper [*Peysson et al.*, 1999].

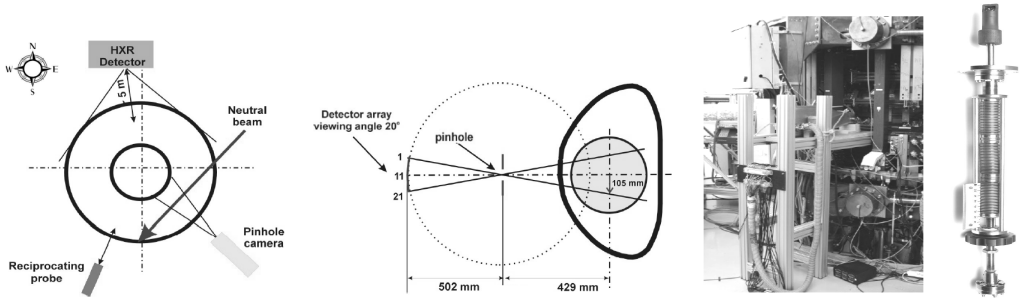

Figure 1. (a) Scheme of experimental setup — top view. (b) Poloidal view. Observing angle was $\approx 30°$ covering the central part of circular plasma column. (c) Photo of 21 pinhole camera at COMPASS Tokamak. (d) Photo of the Cherenkov detector outside the tokamak.

Cherenkov detector

In collaboration with Polish National Centre for Nuclear Research we have tested during autumn 2012 Cherenkov radiation scintillation detector. The detector is made from AlN polycrystals with a diameter of 10 mm and thickness of 1 mm. Collecting surface is about 3 mm^2. The detector is placed inside tokamak vessel on a fixed manipulator and the emitted Cherenkov radiation is transferred to a photomultiplier by optical cable. Detectable energy range is from 70 keV to $\approx$ 1 MeV but without a possibility for an absolute calibration. Advantage of this method is a well defined determination of the position of runaway electrons. The drawback of this method is the need for a separate port which are generally scarce. More information about the detector can be found in [*Plyusnin et al.*, 2010].

Energy calibrations

We have performed an energy calibration of both HXR detectors by a radiative source Cesium 137 which is the source of a monochromatic radiation at 661.7 keV. Scintillation detector gave a clear peak in energy spectrum from which we have computed the calibration constant to be 5.1 MeV/1 V. Calibration of 21 pinhole camera was much more difficult because the low stopping efficiency and Compton scattered photons from shielding box completely smoothed out the peak of Cesium 137. Only from energy conservation argument we have determined the calibration constant to be roughly 250 keV/1 V, a value comparable to that found in the paper of *Peysson et al.* [1999] on page 3998. Calibration of Cherenkov detector is not practically possible so the measured values of runaway electrons energy have to be inferred from other diagnostics.

Experimental setup

A schema of an experimental setup is shown in Figure 1. Scintillation detector is placed north of the tokamak vessel in a 2.5 m height. 21 pinhole camera was placed outside of the tokamak chamber behind the port covered by a 15 mm thick stainless steel flange, later it was moved to observe HXR radiation directly through the vessel wall and the whole poloidal cross section of plasma column without substantial changes in measured signals. Cherenkov detector was placed at the south-east port of tokamak COMPASS.

Measurements results

Low density D-shape discharge

First we show measurement of a typical low density D-shape SNT plasma discharge #4147 with a flat top plasma current $\approx$ 200 kA (see Figure 2a). On both diagnostics we observe large HXR activity caused by runaway electrons. Maximal energy of incoming photons is stable during whole discharge and is about 1 MeV, the same on both diagnostics. While during the flat-top phase the signal is similar on both diagnostic, at the beginning and mainly during the ramp down phase we see large difference between the two diagnostics caused by the presence of limiters or asymmetry of plasma column with respect to the vessel. The scintillation detector detect photons with energy up to 4 MeV at ramp down phase. As will be shown later the theoretical value of runaway energy could be even higher so the linear response of the detector in this high energy range can be questioned.

From energy histogram we can estimate effective temperature of the hottest tail (> 100 keV) of runaway electron population to be ≈ 300 keV. Unfortunately we have not observed no vertical inhomogeneity in different channels of the 21 pinhole camera. This fact is caused by the wall acting as an averaging media, i.e., the wall scatters photons from all places of the vessel and therefore smooths out any vertical inhomogeneity possibly existing in plasma. The same effect was observed, e.g., in Tore Supra tokamak [*Bizarro*, 1993].

Discharge with Neutral Beam Injection

As a next interesting experimental observation we show typical plasma discharge #4167 with a Neutral Beam Injection (NBI) heating. In the NBI discharges there is a high density so no HXR emission stemming from runaway electrons is observed. On the other hand we have observed immediate onset of the HXR signal with the start of NBI heating. Neutral deuterium particles are injected with average energy of 40 keV and all other plasma particles are supposed to have lower energy. The only reasonable explanation for the observation of ≈ MeV photons is interaction of charged D–D fusion products with the vessel wall

$$D + D \mapsto p(3.0\ \text{MeV}) + T(1.0\ \text{MeV}) \tag{1}$$

$$D + D \mapsto He(0.82\ \text{MeV}) + n(2.45\ \text{MeV}) \tag{2}$$

The ratio of the two reactions is 1:1. The observed energy spectra with two components (see slopes in Figure 4b) support this explanation. We observe slower HXR decay after the end of NBI operation, which could be used for estimates of slowing down rate of fast D^+ ions in plasma or the lost rate from plasma. The total number of fusion reactions can be also made. There are $\approx 10^4$ peaks in the HXR signal, so by the same procedure as explained in the subsection 'Number of runaway electrons' we can arrive to a total number $\approx 10^{10}$ of fusion reactions per shot, i.e., ≈ 70 ms of 'active phase.' These number is in disagreement with a number predicted by the code Fafner 10^{13} reactions per second performed for the State Office for Nuclear Safety [private communication with Jakub Urban]. This can be explained by the fact that majority of fusion products remains and thermalize in the plasma. However this disagreement should be studies in closer detail in the future. From Figure 4b) we can also see that L-H transition had no substantial effect on HXR signal or on fusion products confinement.

Interaction of Runaway Electrons with reciprocating probe

We have observed two interesting effects during operation of horizontal reciprocating probe. The scintillation detector, which is located on the opposite side of tokamak vessel, encountered no change in HXR signal during insertion of the horizontal probe into the plasma. But 21 pinhole camera which was located in the vicinity of reciprocating probe measured local amplification of measured HXR signal when the probe head approached the plasma (see Figure 3a) and on the other hand total local suppression of HXR signal (Figure 3b) when the probe went deeper into the plasma behind separatrix (as follows from the shape of the plasma potential measured by the probe). It seems that the probe head acts as limiter in the later case while in the first case it perturbs trajectories of runaway electrons so they preferentially hit the wall near the 21 pinhole camera. Explanation that photons come from interaction with the probe is also possible, but to get final answer to explain this behavior further experiments will be needed.

Measurements with Cherenkov detector

In Figure 5 we show results of simultaneous measurements of the Cherenkov detector and the NaI scintillation detector. Again, as in previous measurements, we can clearly see apparent toroidal asymmetry between the two signals. While the Cherenkov detector is clearly not in some limiter shadow, the deposition pattern and preferential area where runaway electrons hit the inner parts of vessel is located in the northern part of the tokamak vessel.

Theoretical predictions and consistency considerations

Number of runaway electrons

We have counted peaks in the scintillation detector signal in shot #4116 to be $\approx 10^5$. Assuming that HXR is radiated isotropically into full spatial angle we can estimate total number of runaway electrons created during the discharge. Collecting area of the scintillation detector is ≈ 5 cm^2 and surface of 5 m sphere is $S = 4\pi(500\ \text{cm})^2 \approx 3 \cdot 10^6$ cm^2. The ratio of the detected to all created runaway electrons is roughly 10^{-6}, so the estimated total number of runaway electrons is $N_{RE-scintillator} \approx 10^5 \cdot 10^6 = 10^{11}$.

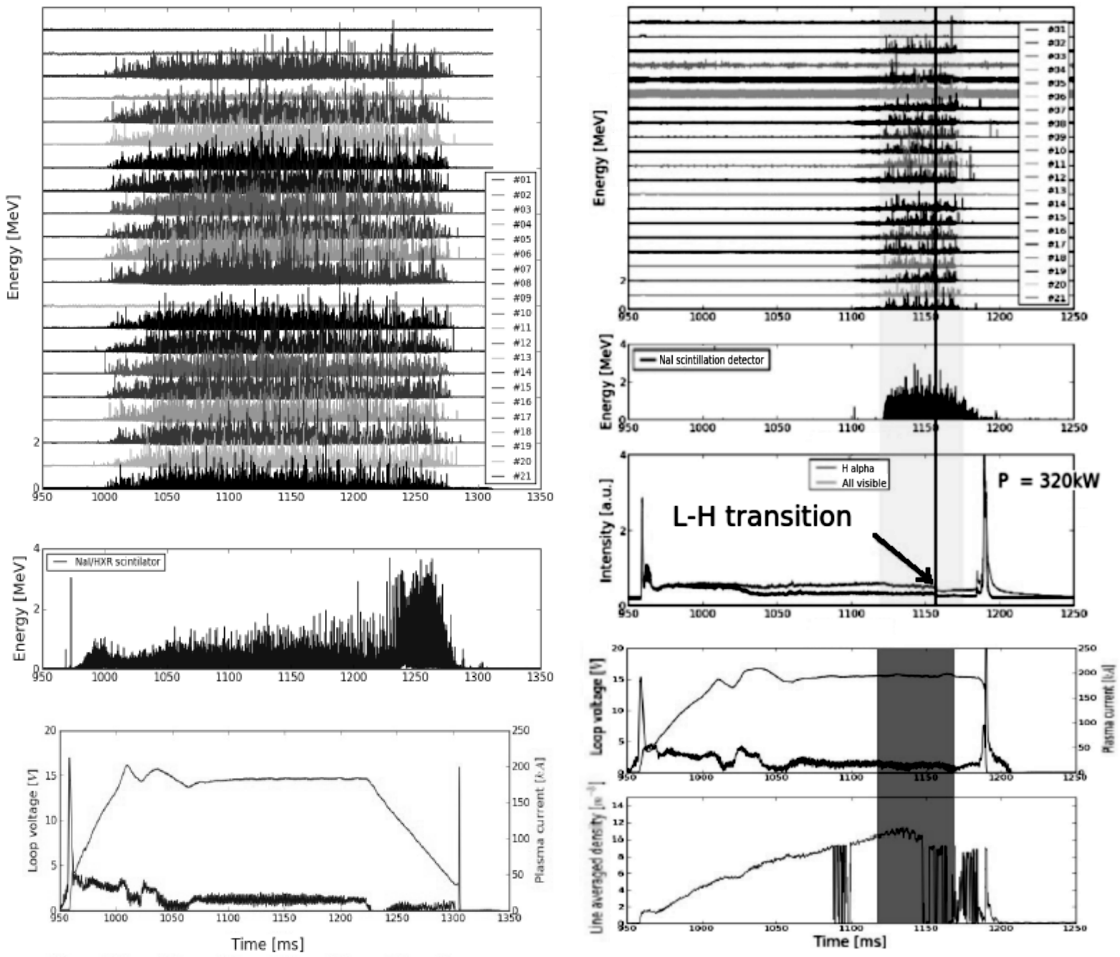

Figure 2. (a) HXR signals as measured by 21 pinhole CdTe semiconductor array of detectors in shot #4147. In the middle HXR signal from NaI scintillation detector placed in a 5 m distance from tokamak vessel. Time evolution of plasma current and loop voltage during the shot #4147. (b) The same quantities as in the left figure for shot #4167 with Neutral Bean Injection heating. Operation of NBI is indicated by colored areas in the plots.

The COMPASS tokamak has a Thomson scattering diagnostic which provides time evolution of radial profiles of electron density and electron temperature measured on the vertical axis. Assuming approximatively radially constant toroidal electric field corresponding to the measured loop voltage we can predict local runaway electron production rate. There are many theoretical papers dedicated to derivation of correct expression for the production rate [see, e.g., review paper *Knoepfel and Spong*, [1979]) as well as some numerical codes computing production rate [e.g., ARENA, CQL3D]. Historically later expressions for production rate have similar form differing usually only in a numerical factor. For our study we have chosen Kruskal-Bernstein expression [e.g., *Helander et al.*, 2002]

$$\frac{dn_r}{dt} = \frac{dn_r}{dt} = kn_e\nu_{ee}\epsilon^{-3(1+Z)/16}exp(-\frac{1}{4\epsilon} - \sqrt{\frac{1+Z}{\epsilon}}) \tag{3}$$

where k is a factor of order unity, $\nu_{ee} \sim \frac{n_e}{T_e^{3/2}}$ collisional frequency and $\epsilon = |E_{||}|/E_D << 1$. E_D is well known Dreicer critical electric field $E_D = \frac{e^3 ln\Lambda}{4\pi\epsilon^2}\frac{n_e}{T_e}$. As shown in Figure 6 typical operating areas of tokamak COMPASS give value of Dreicer electric field to be in the range 10–100 V·m^{-1}. For a typical COMPASS loop voltage 1 V·m^{-1} is $\epsilon < 0.03 << 1$. Functional dependence of runaways production rate on parameter $\epsilon \sim E_{||}n_e/T_e$ is shown in Figure 6b from which we can see how enormously sensitive is theoretical formula for runaways production for the relevant ϵ range values. For example 20 % decrease in density changes production rate by one order of magnitude and it is similar for electric field or electron temperature.

In Figure 7 we show data from Thomson scattering diagnostic and the measured loop voltage for typical low density discharge #4116. From Figure 7 we see that runaways production rate has

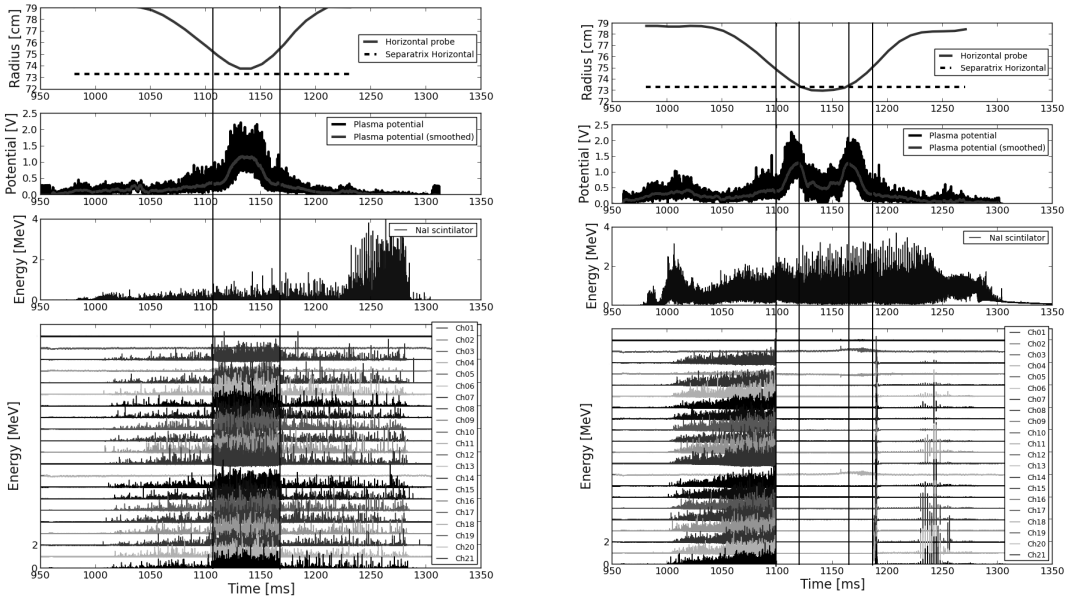

Figure 3. (a) In the top plot there is the head position of the horizontal reciprocating probe and the measured plasma potential with respect to time. From the shape of plasma potential we deduce that the probe did not cross the separatrix. While HXR signal of scintillation detector shows no change with respect to the operation of the probe, 21 pinhole camera exhibit large amplification closely correlated with approaching the probe towards the plasma. Shot #4154. (b) From the shape of the plasma potential we deduce that the probe crossed the separatrix. HXR signal of 21 pinhole camera shows complete suppression while the signal of scintillation detector remains generally unchanged. Shot #4159.

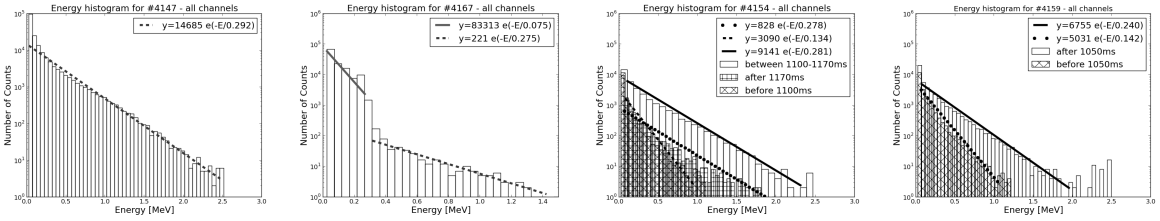

Figure 4. Photon energy histograms for shots (a) #4147 (b) #4167 (c) #4154 and (d) #4159.

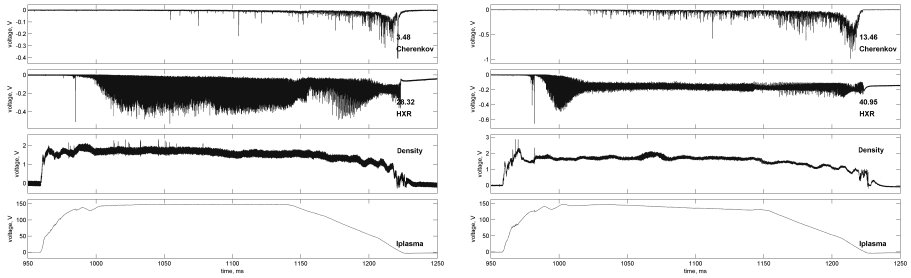

Figure 5. (a) Circular discharge #3744. (b) Low density D-shape discharge #3752.

approximatively average value equal to 10^{13} m^{-3}·s^{-1}. Volume of the plasma core is ≈ 0.1 m^3 and time when runaway electrons are created is ≈ 0.2 s. This gives another estimate of the total number of runaway electrons created during the discharge $N_{RE-Thomson} \approx 0.1$ m$^3 \cdot 10^{13}$ m^{-3}·s$^{-1} \cdot 0.2$s$= 10^{11}$.

We see that the two different methods gives roughly the same estimate of the number of runaway electrons created during the discharge.

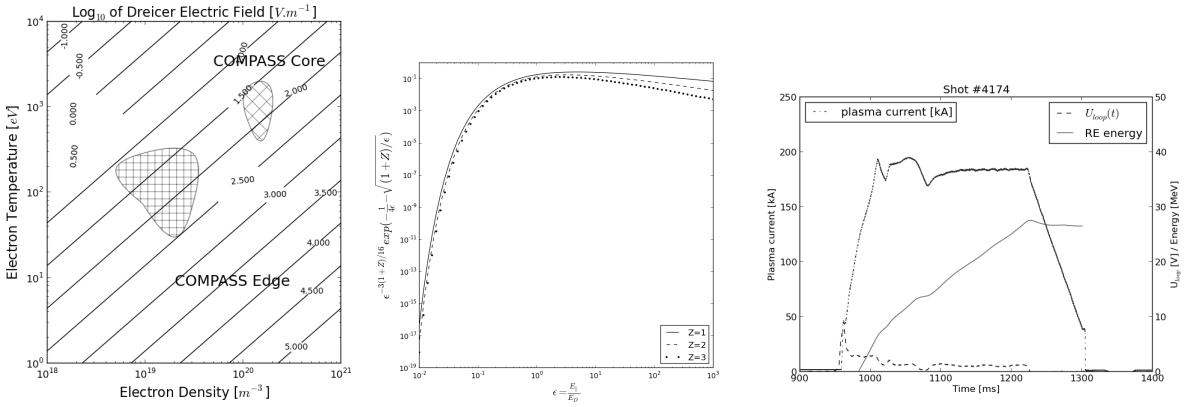

Figure 6. (a) Dependence of Dreicer electric field on temperature and density. Typical operating parameters of the COMPASS tokamak in the plasma core/edge are red/blue areas. (b) Plot of function $\epsilon^{-3(1+Z)/16} exp(-\frac{1}{4\epsilon} - \sqrt{\frac{1+Z}{\epsilon}})$. (c) Time evolution of runaway electron energy ideally accelerated by toroidal electric field corresponding to the measured loop voltage.

Current carried by runaway electrons

Runaway electron current, making an assumption that runaway electrons move practically with the speed of light and their trajectory is approximately a circle with a tokamak major radius, is given by a simple formula

$$I_{RE} = \frac{ecN_{RE}}{2\pi R_0} \tag{4}$$

where $R_0 = 0.55$ m is the COMPASS major radius. Therefore runaway current in the COMPASS shot #4116 is ≈ 1 A assuming $N_{RE} \approx 10^{11}$. Or ≈ 1 kA assuming less probable number of runaways $N_{RE} \approx 10^{14}$, but still possible in reality.

Energy of runaway electrons

Making assumption that the runaways are not decelerated by any force (collisional drag is small, breaking by radiation is small until energy ranges of a few tens of MeVs) and assuming that the electrons have the speed of light we can compute their energy $W(t)$ acquired by accelerating toroidal electric field by the expression

$$W(t) = \int F_e(t)dx = e\int E_{toriodal}(t)cdt = \int ecE_{toriodal}(t)dt \tag{5}$$

where $E_{toriodal} = \frac{U_{loop}}{2\pi R_0} \approx 0.3$ V m^{-1}. In Figure 6c we show the an ideal time evolution of runaway electron energy during shot #4174. From this calculation we can see that theoretically the runaway electron can get energy up to ≈ 20 MeV in this discharge. On the other hand from scintillator detector measurement (Figure 7b) we estimate the maximum energy to be around 5 MeV. This inconsistency can be caused by non-linear response of scintillation detector in this energy high range and we should bear it in mind in future considerations.

Taking the energy estimate of runaways to be ≈ 10 MeV we can estimate a total energy carried by runaways: $E_{RE} = N_{RE} \cdot E_{REaverage} \approx 10^{11} \cdot 10$ MeV$\cdot 10^{-19}$ J/eV$= 0.1$ J. This energy is very small compared to the total plasma energy in the discharge ≈ 1 kJ so the runaways should not have a substantial influence on the plasma discharge dynamics in this case.

Discussion and Conclusion

In this paper we have presented an evidence of the observation of runaway electrons and fusion products by three different types of diagnostics at the COMPASS tokamak. The NaI scintillator detector gives the most reliable information about energy spectra, but almost no spatial information about runaways. On the other hand the Cherenkov detector gives information with excellent spatial localization and good energy distribution but without practical possibility of an absolute calibration. Energy spectra determined from 21 pinhole camera are severely influenced by several factors, namely the very

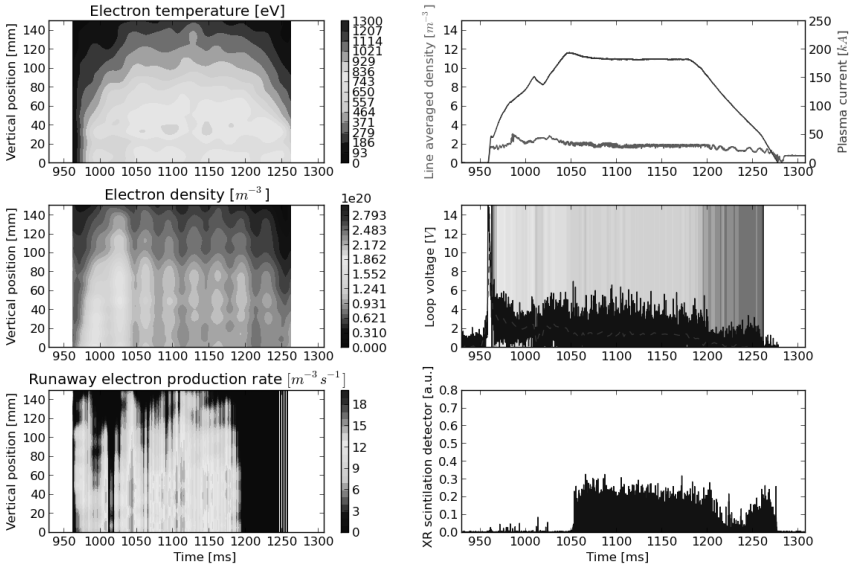

Figure 7. Profiles of electron temperature and density from Thomson scattering, loop voltage and computed runaway electrons production rate for the shot #4116.

low stopping efficiency of low volume semiconductor detectors and insufficient shielding box for highly energetic photons. At the same time the spatial resolution is adversely influenced by the presence of the tokamak vessel which almost completely destroys the spatial information.

By measurements we have found the evidence that runaways are present in the COMPASS tokamak with energies at least up to $\approx$ 4 MeV. Energy spectra for some discharges are depicted in series of Figures 4a–c. The theoretical calculation showed that actual maximal energies of runaway can be even higher by a factor of 2–4. This discrepancy can be caused by a non linear response of detectors in high energy range and should be tested, e.g., by radiation sources with calibration sources with higher energy than Cesium 137.

We have estimated number of runaway electrons in shot #4116 by two different methods. First based on the number of measured counts by the scintillation detector, second by the use of measured density and temperature profiles from Thomson scattering and loop voltage. This two methods give the same order of magnitude estimate for runaways created. The number of runaway electrons typically produced in the tokamak COMPASS low density discharges is $\approx 10^{11}$. Based on this number the runaway current is ≈ 1 A and energy carried by runaways ≈ 0.1 J.

Acknowledgments. The authors thank to CEA Cadarache, France for the lending of the 21 pinhole HXR camera and National Centre for Nuclear Research, Department of Plasma Physics and Materials Engineering, Otwock, Poland for collaboration on measurements with Cherenkov detector. This work was supported by the Academy of Sciences of the Czech Republic IRP #AV0Z20430508, the Ministry of Education, Youth and Sports CR #7G10072 and #LA08048 and European Communities under the contract of Association between EURATOM/IPP.CR No. FU07-CT-2007-00060. The views and opinions expressed herein do not necessarily reflect those of the European Commission.

References

Bizarro, J. P., Peysson, Y., Bonoli, P. T., et al., On self-consistent ray-tracing and Fokker-Planck modeling of the hard x-ray emission during lower-hybrid current drive in tokamaks, *Phys. Fluids B* 5(9), 1993.

Helander, P., Eriksson, L.-G. and Andersson, F., Runaway acceleration during magnetic reconnection in tokamaks, *Plasma Phys. Control. Fusion* 44, 247–262, 2002.

Ikeda, K. *et al.*, Progress in the ITER Physics Basis, *Nuclear Fusion*, 47(6), 2007.

Knoepfel, H., Spong, D.A., Runaway electrons in toroidal discharges, *Nuclear Fusion*, 19, 785, 1979.

Peysson, Y., and F. Imbeaux, Tomography of the fast electron bremsstrahlung emission during lower hybrid current drive on TORE SUPRA, *Rev. Sci. Instrum.*, 70(10), 1999.

Plyusnin, V. V., Jakubowski, L., Zebrowski, J., Duarte, P., Characteristics of four-channel Cherenkov-type detector for measurements of runaway electrons in the ISTTOK tokamak, *Rev. Sci. Instrum.*, 81(10), D304, 2010.